Original Article
Prostate diseases and male voiding dysfunctions

pISSN: 2287-4208 / eISSN: 2287-4690
World J Mens Health 2022 Jan 40(1): 149-161
https://doi.org/10.5534/wjmh.200204

The World Journal of MEN's HEALTH

Circ_0001686 Promotes Prostate Cancer Progression by Up-Regulating SMAD3/TGFBR2 *via* miR-411-5p

Jiancheng Pan*, Zihao Liu*, Zhizhao Yang, Enli Liang, Cheng Fang, Dingrong Zhang, Xiaodong Zhou, Yuanjie Niu, Zhongcheng Xin, Yegang Chen, Qiliang Cai*

Department of Urology, the Second Hospital of Tianjin Medical University, Tianjin Institute of Urology, Tianjin, China

Purpose: As the mechanism of interaction between circular RNAs (circRNAs) and microRNAs (miRNAs) in regulating the development of prostate cancer (PCa) is not clear, this study focuses on investigating these effects.

Materials and Methods: Sample tissues were collected from the PCa of patients, and microarray analysis of human circRNAs was conducted. The expression of circ_0001686, hsa_miR-411-5p (miR-411-5p) were also detected by qRT-PCR. Circ_0001686 and miR-411-5p mimics were transfected into the PCa cell lines (CWR22RV1and LNCaP) and MTT, colony formation, Transwell, and scratch wound assays were used to analyze the biological behaviors of PCa cells. Si-circ_0001686 and ASO-miR-411-5p were used as negative controls, and dual-luciferase reporter assays were performed to verify the interactions among circ_0001686, miR-411-5p, and SMAD3/TGFBR2. The levels of SMAD3 and TGFBR2 in different treated PCa cells were measured by western blot, and *in vivo* experiments in a nude mouse model were carried out to strengthen the *in vitro* findings of miR-411-5p.

Results: The expression of circ_0001686 was up-regulated, while the expression of miR-411-5p was down-regulated in PCa cells. Moreover, circ_0001686 promoted cell proliferation, migration, and invasion. Molecular mechanism exploration revealed that circ_0001686 could reduce miR-411-5p, affecting the downstream target genes of SMAD3 and TGFBR2. *In vitro* and *in vivo* studies verified that miR-411-5p inhibits PCa progression.

Conclusions: Circ_0001686 can reduce miR-411-5p to increase the expression of SMAD3/TGFBR2, which consequently promotes the proliferation, invasion, and migration of PCa cells.

Keywords: CircRNA; miRNA; Prostate cancer

Received: Jan 20, 2021 **Revised:** Feb 28, 2021 **Accepted:** Mar 2, 2021 **Published online** May 18, 2021

Correspondence to: Yegang Chen https://orcid.org/0000-0002-1984-3695
Department of Urology, the Second Hospital of Tianjin Medical University, Tianjin Institute of Urology, Tianjin 300211, China.
Tel/Fax: +86-8832-8603, **E-mail:** yegangchen@tmu.edu.cn
Co-Correspondence to: Qiliang Cai https://orcid.org/0000-0002-4273-0103
Department of Urology, the Second Hospital of Tianjin Medical University, Tianjin Institute of Urology, Tianjin 300211, China.
Tel/Fax: +86-8832-6501, **E-mail:** caiqiliang@tmu.edu.cn
*These authors contributed equally to this work as co-first authors.

INTRODUCTION

Prostate cancer (PCa) is the most common non-epidermal cancer in male worldwide [1]. Despite significant improvements in the screening, diagnosis, and treatment, the overall survival rates in PCa remain poor [2]. Several genes have been associated with the development of PCa, but their molecular mechanism in cancer progression is not yet completely understood [3]. Therefore, it is critical to elucidate the genetic mechanisms that could improve our understanding of the pathogenesis of PCa.

Circular RNAs (circRNAs) have characteristics of covalently closed-loop structures and are a new class of non-coding RNAs (ncRNAs) that do not code for proteins [4,5]. Recently, circRNAs have attracted greater attention due to their role in tumor progression [6] and have been implicated in regulating tumorigenesis in several cancers, including gastric cancer [7], breast cancer [8], and colorectal cancer [9,10]. Considerable evidence now also suggests that an increasing number of circRNAs are associated with the development and progression of PCa [3,11,12]. However, there is a lack of scientific information regarding their expression specificity and sensitivity when used as PCa biomarkers.

Like long ncRNAs (lncRNAs), circRNAs can also interact with microRNAs (miRNAs) [13]. By directly binding to the 3'-untranslated regions of their target genes, miRNAs regulate gene expression, cause messenger RNA (mRNA) cleavage, or lead to translational inhibition of their targets [14]. In this way, miRNAs significantly affect cell growth, apoptosis, migration, and carcinogenesis [15]. Thus, elucidating cancer-specific miRNAs' roles is necessary [16], and several miRNAs have been identified as tumor suppressors. Our previous circRNA microarray analysis found that circ_0001686 was differentially expressed in PCa and normal tissues and that miRNA-411-5p was a possible target gene through the Starbase (http://starbase.sysu.edu.cn/). Studies have found that miR-411-5p can inhibit the growth and metastasis of bladder cancer by targeting the zinc transporter 1 (ZnT1) protein [17], although the role of miR-411-5p in PCa is still unknown. Using Starbase, we found that miRNA-411-5p could regulate several target protein genes, and because transforming growth factor-beta (TGF-β) signaling pathway plays an important role in the progression of PCa and TGFBR2 and SMAD3 are its key proteins [18], we used TGFBR2 and SMAD3 as the putative targets of miR-411-5p. In doing so, we put forward a hypothesis that circ_0001686 could interact with miR-411-5p which regulates TGFBR2/SMAD3 and subsequently leads to PCa tumor growth.

MATERIALS AND METHODS

1. Ethics statement

Experients were performed under a project license (NO.: KY2020K061) granted by the Second Hospital of Tianjin Medical University, in compliance with national guidelines for the care and use of animals. Written informed consent was obtained from each patient.

2. Patients and tissue specimens

PCa tissue samples and adjacent normal tissues were collected from 30 PCa patients at the Second Hospital of Tianjin Medical University from March 2018 to October 2019. No patient received chemotherapy or radiotherapy before surgery. All tissue specimens were stored at -80℃ until used for RNA extraction.

3. CircRNAs microarray analysis

Microarray assays were carried out to screen the differential expression of circRNAs between three PCa tumors and adjacent normal tissues. RNA extraction and microarray hybridization were performed per Arraystar's standard protocols described previously [3].

4. Differential expression profile analysis of circRNAs

The linear models identified the differentially expressed circRNAs between the normal tissue and PCa tissue groups for Microarray Data (LIMMA, http://www.bioconductor.org/packages/release/bioc/html/limma.html) package in R language. False positives were removed based on the adjusted p-values using the Benjamini and Hochberg false discovery rate method. An adjusted p-value<0.05 and |logFC| ≥1 were the cut off criterion.

5. Cell culture

Human prostate epithelial cell line RWPE1 and PCa cell lines (CWR22RV1 and LNCaP) were obtained from Cosmo Bio (Cosmobio., Tianjin, China) and were cultured in RPMI-1640 (Gibco-BRL, Rockville, MD, USA) supplemented with 10% fetal bovine serum (FBS) and 1%

streptomycin/penicillin in a 5% (v/v) CO_2 incubator at 37℃.

6. RNA transfection

CWR22RV1 and LNCaP cells (2×10^5 cells) were cultured with the antibiotic-free complete medium in six-well plates, then transfected with pcDNA3.1/circ_0001686 or pcDNA3.1/NC, and si-circ_0001686 or si-NC, correspondingly. Transfection was carried out using Lipofectamine 3000 (Invitrogen, Carlsbad, CA, USA) as per the manufacturer's protocol. The pcDNA3.1/circ_0001686 and si-circ_0001686 were synthesized by GenePharma (Shanghai, China). For miRNA transfection, the miR-411-5p mimics (5′-AUCACAUUGCCAGGGAUUUCC-3′), miR-411-5p mimics NC (5′-UUCUCCGAACGUGUCACGUTT-3′), a miR-411-5p antisense oligonucleotide (ASO-miR-411-5p, 5′-GUGGUAAUCCCUGGCAAUGUGAU-3′, and ASO-NC (5′-CAGUACUUUUGUGUAGUACAA-3′) were obtained from Sangon Biotech Co., Ltd. (Shanghai, China). Cells (1×10^5 cells/well) were seeded in six-well plates and transfected with miR-411-5p mimics, mimics NC, ASO-miR-411-5p, and ASO-NC, correspondingly using Lipofectamine 3000 reagent (Thermo, Waltham, MA, USA) as per the manufacturer's protocol. The cells were harvested for further experiments after 48 hours of transfection.

7. RNA extraction and quantitative RT-PCR

Total RNA from cells was extracted using TRIZOL reagent (Invitrogen), and the Reverse Transcription System Kit (TaKaRa, Dalian, China) reverse-transcribed RNA into cDNA. The qRT-PCR reactions were performed using the ABI7500 System and SYBR Green PCR Master Mix (TaKaRa), and the primers sequences used in the experiments were as following: (1) hsa_circ_0001686: Forward, 5′-CTAGGAGTCACAGGAAGACATC-3′; Reverse, 5′-GTAGATCTCTCAGACTAGGTTG-3′; (2) SMAD3-F: 5′-GCCCAGTGCCTAAGTGAT-3′; (3) SMAD3-R: 5′-ACACTGAGCCAGAAGAGC-3′; (4) TGFBR2-F: 5′-GGAATGTCTTGGGCAAATCT-3′; (5) TGFBR2-R: 5′-ACCTGAATGCTTGTGCTTTTATT-3′; (6) β-ACTIN-F: 5′-CCACATCGCTCAGACACCAT-3′; (7) β-ACTIN-R: 5′-ACCAGGCGCCCAATACG-3′; (8) miR-411-5p-F: 5′-GGGCTTAATGCTAATTGTGAT-3′; (9) miR-411-5p-R: 5′-CAGTGCGTGTCGTGGAGT-3′; (10) hsa-U6-F: 5′-AAAGACCTGTACGCCAACAC-3′; and (11) hsa-U6-R: 5′-GTCATACTCCTGCTTGCTGAT-3′. These primers were obtained from GenePharma. The relative expression levels were measured using the $2^{-\Delta\Delta Ct}$ method [19].

8. Western blotting

Total protein from the cells was extracted using RIPA lysis buffer (Sigma, St. Louis, MO, USA), and the protein samples were separated using a 10% sodium dodecyl sulfate-polyacrylamide gel electrophoresis (SDS-PAGE) and then transferred onto a polyvinylidene difluoride membrane. Membrane blocking with 5% non-fat milk for 2 hours followed, and the membranes were then incubated overnight at 4℃ with the corresponding primary antibodies: anti-GAPDH (1:1,000; ab181602; Abcam, Cambridge, UK), anti-SMAD3 (phospho S467) (1:1,000; ab52903; Abcam), anti-p-SMAD3 (1:1000; ab92547; Abcam), and anti-TGFBR2 (1:1,000; ab186838; Abcam). After washing three times, membrane incubation with peroxidase-labeled secondary antibody (anti-rabbit IgG, 1:2,000; ab6721; Abcam) was carried out for 2 hours. Enhanced chemiluminescence (Thermo) was used to visualize the protein bands, and analysis was carried out using Image Lab™ Software (Bio-Rad, Hercules, CA, USA).

9. MTT assay

Briefly, the transfected cells (1,000 cells/well) were plated into 96-well plates, adhered overnight, and cultured at 37℃ in 5% CO_2. Then, at 0 and 48 hours, 20 μL of 5 μg/mL MTT (3-(4,5-dimethylthiazol-2-yl)-2,5-diphenyl tetrazolium bromide) solution in PBS was added to each well. After 4 hours of incubation, the formazan crystals were dissolved by adding 100 μL of 10% SDS. Finally, absorbance was measured at 490 nm using a microplate reader (Bio-Rad).

10. Colony formation assay

For the colony formation assay, the transfected CWR22RV1 and LNCaP cells (200 cells/well) were seeded in 12-well plates. After 7 days, the cells were stained with crystal violet, and the colony formation ability was evaluated by the average colony count.

11. Transwell assay

For cell invasion analysis, Transwell chambers (Corning, Corning, NY, USA) were used to perform the Transwell assay. 200 μL of cells (0.1×10^6) were seeded in the upper chamber, which was pre-coated with matri-

gel, while 600 μL of DMEM containing 10% FBS was placed in the lower chamber. After 24 hours of incubation at 37°C, cells transversed to the lower chamber were fixed in 1% formaldehyde and stained with 0.1% crystal violet. Both fixing and staining procedures were carried out for 20 minutes each, and positively stained cells were observed and counted at three randomly selected fields under a microscope (Olympus, Beijing, China).

12. Scratch wound assay

The transfected cells (CWR22RV1 and LNCaP) were seeded into 12-well plates for the cell migration analysis. A 200 mL pipette tip was then used to scratch the cell layers, and these were maintained in DMEM with 10% FBS. The cells were photographed to record the wound width at 0 and 48 hours in an inverted microscope.

13. Cell apoptosis analysis

Cell apoptosis was measured using the Annexin V-FITC kit (Biosea, Beijing, China). For this, cells (5.0×10^5 cells/mL) resuspended in PBS buffer were subsequently double-stained with Annexin V-Alexa Fluor 647 and propidium iodide. Finally, the cell apoptotic rate was measured using a flow cytometer (BD Biosciences, San Diego, CA, USA).

14. Flow cytometry analysis of CD44 expression

CD44 expression on prostate cells was evaluated using flow cytometry. Experiments were performed with FITC-conjugated mouse anti-human CD44 antibodies (BD Biosciences) using a FACS Canto II instrument (BD Biosciences). Data were analyzed with Cell Quest software (BD Biosciences).

15. Dual-luciferase reporter assay

Binding interaction was predicted using the Starbase. The pmirGLO vectors with wild type or a mutant miR-411-5p binding site in circ_0001686 3'-UTR were constructed. The 3'-UTR sequences of SMAD3 and TGFBR with corresponding binding sites for miR-411-5p were cloned into the pmirGLO3 reporter vectors (Promega, Madison, WI, USA) to generate the wild-type pmirGLO-SMAD3 (pmirGLO-SMAD3 wt) and the wild-type pmirGLO-TGFBR (pmirGLO-TGFBR wt) plasmids. Mutant reporter plasmids, mutant-type pmirGLO-SMAD3 (pmirGLO-SMAD3 mut), and mutant-type mirGLO-TGFBR reporter (pmirGLO-TGFBR mut) were generated using the GeneArt™ Site-Directed Mutagenesis System (Thermo). Corresponding plasmids were transfected using Lipofectamine 3000, and luciferase activity was measured using a dual-luciferase kit (Promega) to perform the luciferase assays.

16. *In vivo* mice model studies

For the *in vivo* tumor studies, 6-week-old BALB/c male nude mice were randomly divided into two groups (nine mice per group) and subcutaneously injected into the right flank CWR22RV1 cells (3×10^6, 200 μL), which were transfected with either miR-411-5p mimics or mimics NC. The growth of the resulting tumors was examined every 7 days. After 4 weeks of inoculation, mice were anesthetized using 1% to 3% isoflurane; then, the tumors were excised to measure weight and volume and photographs taken. The tumor volume was calculated using the formula: Volume=(length×width^2)/2 (mm^3).

17. Statistical analysis

SPSS 22.0 (IBM Corp., Armonk, NY, USA) and GraphPad Prism 7.0 (GraphPad, San Diego, CA, USA) were used to carry out the statistical analyses. The data are presented as the mean±standard deviation from three independent experiments wherever applicable. Student t-test was used to assess the data between the two groups, and the differences between various groups were analyzed by one-way analysis of variance (ANOVA), followed by Tukey's post hoc test and a $p<0.05$ considered to be statistically significant.

RESULTS

1. Differential profiling of circRNAs reveals that circ_0001686 is up-regulated in PCa

Microarray analysis obtained a total of 91 differentially expressed circRNAs comprised of 29 up-regulated circRNAs and 62 down-regulated circRNAs (Fig. 1A). There was a significant difference in Circ_0001686 levels between PCa tumor and healthy tissues, and the expression level of circ_0001686 was markedly higher both in the PCa tissue and PCA cell lines ($p<0.001$, $p<0.01$; Fig. 1B, 1C).

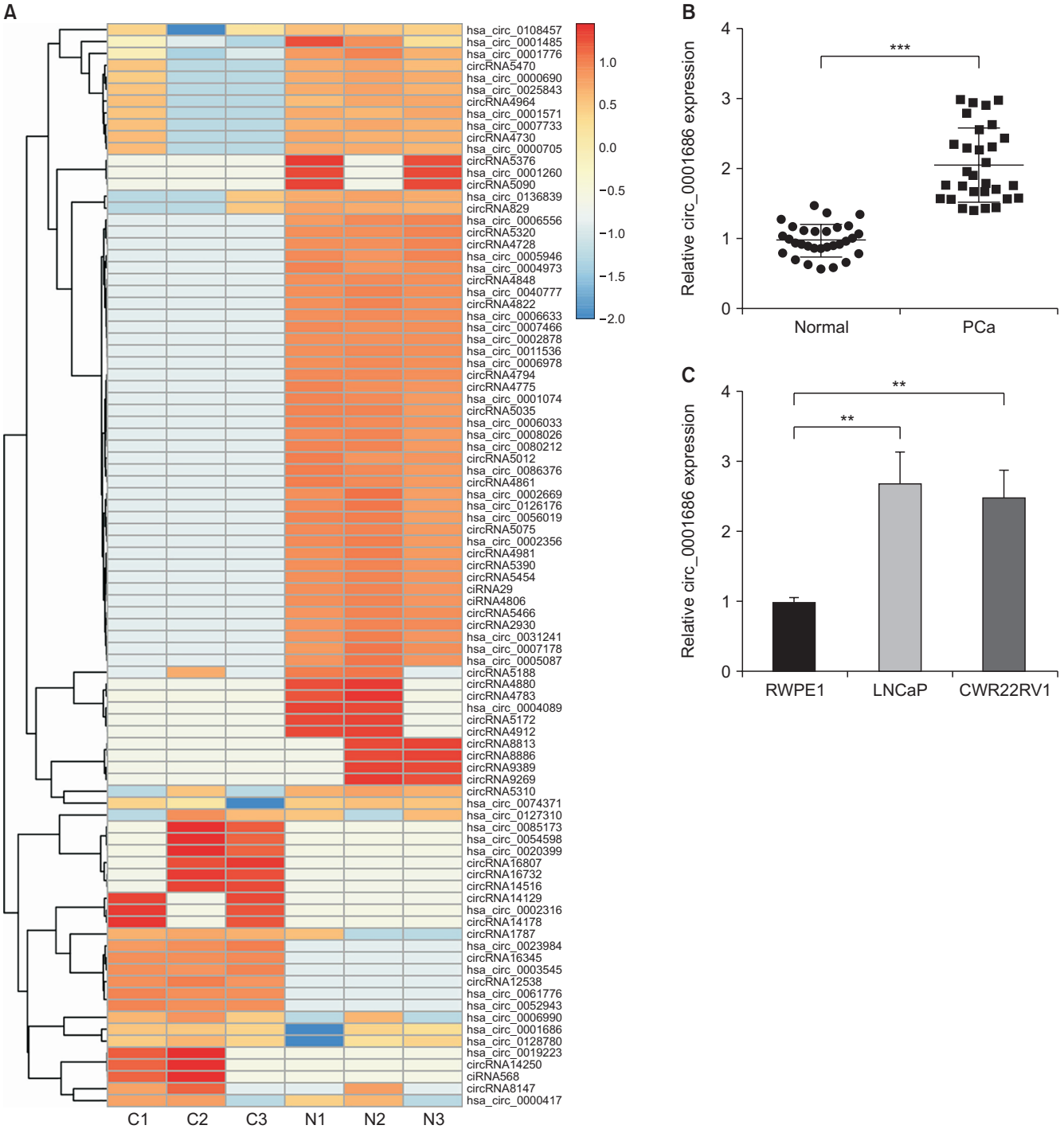

Fig. 1. Differential expression analysis of circRNAs in prostate cancer (PCa) where circ_0001686 was significantly upregulated. (A) The heat map showed the top fifteen most increased and decreased circRNAs in PCa tissues as compared to that in the matched non-tumor tissues analyzed by circRNAs Arraystar Chip. (B) qRT-PCR expression analysis of circ_0001686 in PCa tissue and normal tissue; n=30. (C) qRT-PCR expression analysis of circ_0001686 in PCa (CWR22RV1 and LNCaP) cells. **p<0.01, ***p<0.001.

2. Circ_0001686 promotes the malignant progression of PCa cells

The qRT-PCR results (Fig. 2A) show that circ_0001686 expression increased in pcDNA3.1/ circ_0001686 transfected cells compared with pcDNA3.1/NC transfected cells (p<0.05, p<0.01). The transfection of si-circ_0001686 in CWR22RV1 and LNCaP cells triggered an obvious abatement of circ_0001686 expression, compared to the

The World Journal of MEN's HEALTH

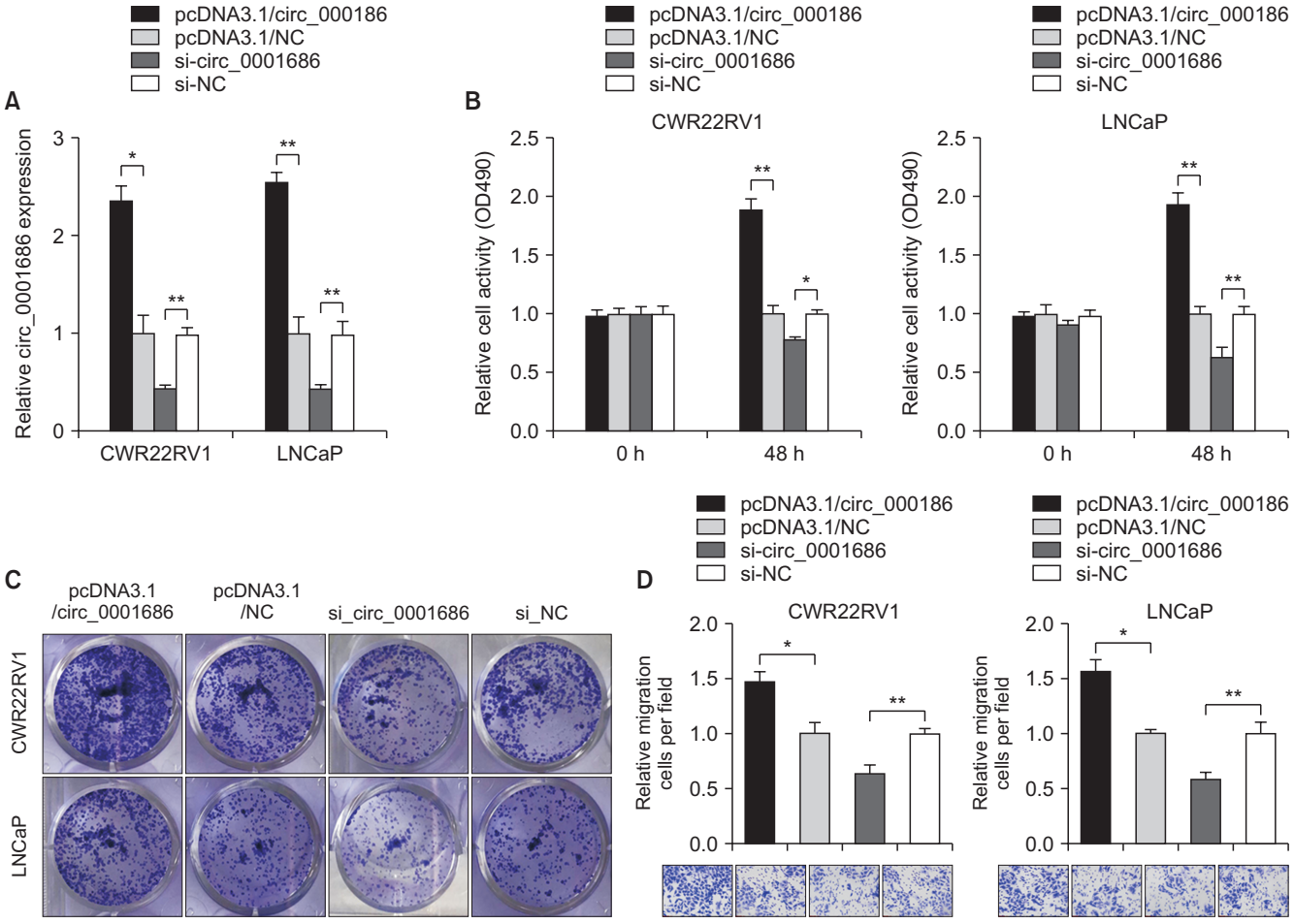

Fig. 2. Circ_0001686 promotes the malignant progression of prostate cancer (PCa) cells. (A) The transfection efficiency measurement of circ_0001686 in the CWR22RV1 and LNCaP cells by qRT-PCR. (B) MTT results of the proliferation of transfected cells at the indicated time points (0, 48 h). (C) Knockdown of circ_0001686 significantly suppressed the colony formation capacity of transfected cells. (D) Transwell assay showed that si-circRNA reduced the migration activity in CWR22RV1 and LNCaP cells (200 μm, ×400). *p<0.05, **p<0.01.

si-NC transfected cells (p<0.01). Furthermore, MTT and colony formation assay indicated that within 48 hours of transfection, circ_0001686 promoted the proliferation of CWR22RV1 and LNCaP cells (p<0.05, p<0.01; Fig. 2B, 2C). In the Transwell assay, pcDNA3.1/circ_0001686 transfection increased CWR22RV1 and LNCaP cells' cell migration abilities, although it was suppressed upon transfection with si-circ_0001686 (Fig. 2D).

3. Circ_0001686 interacts with miR-411-5p in PCa cells

Starbase predicted that circ_0001686 possesses the miR-411-5p seed region. Luciferase reporter assays showed circ_0001686 significantly inhibited luciferase activity of wild-type reporter plasmid having miR-411-5p (Fig. 3A). On the contrary, si-circ_0001686 significantly increased the luciferase activity of wild-type reporters for miR-411-5p. Also, miR-411-5p expression was decreased when tested by qRT-PCR in CWR22RV1 and LNCaP cells (Fig. 3B), and circ_0001686 noticeably suppressed the expression of miR-411-5p in both cells (Fig. 3C).

4. miR-411-5p inhibits the proliferation and invasion of PCa cells

qRT-PCR showed miR-411-5p expression was significantly higher upon transfection with miR-411-5p mimics compared with the mimics NC transfected PCa cells (p<0.05, p<0.01; Fig. 4A) and compared to the ASO-NC group, ASO-miR-411-5p transfection markedly decreased the expression of miR-411-5p (p<0.01; Fig. 4A). MTT and colony formation assay revealed that miR-411-5p significantly repressed the proliferative ability of CWR22RV1 and LNCaP cells within 48 hours

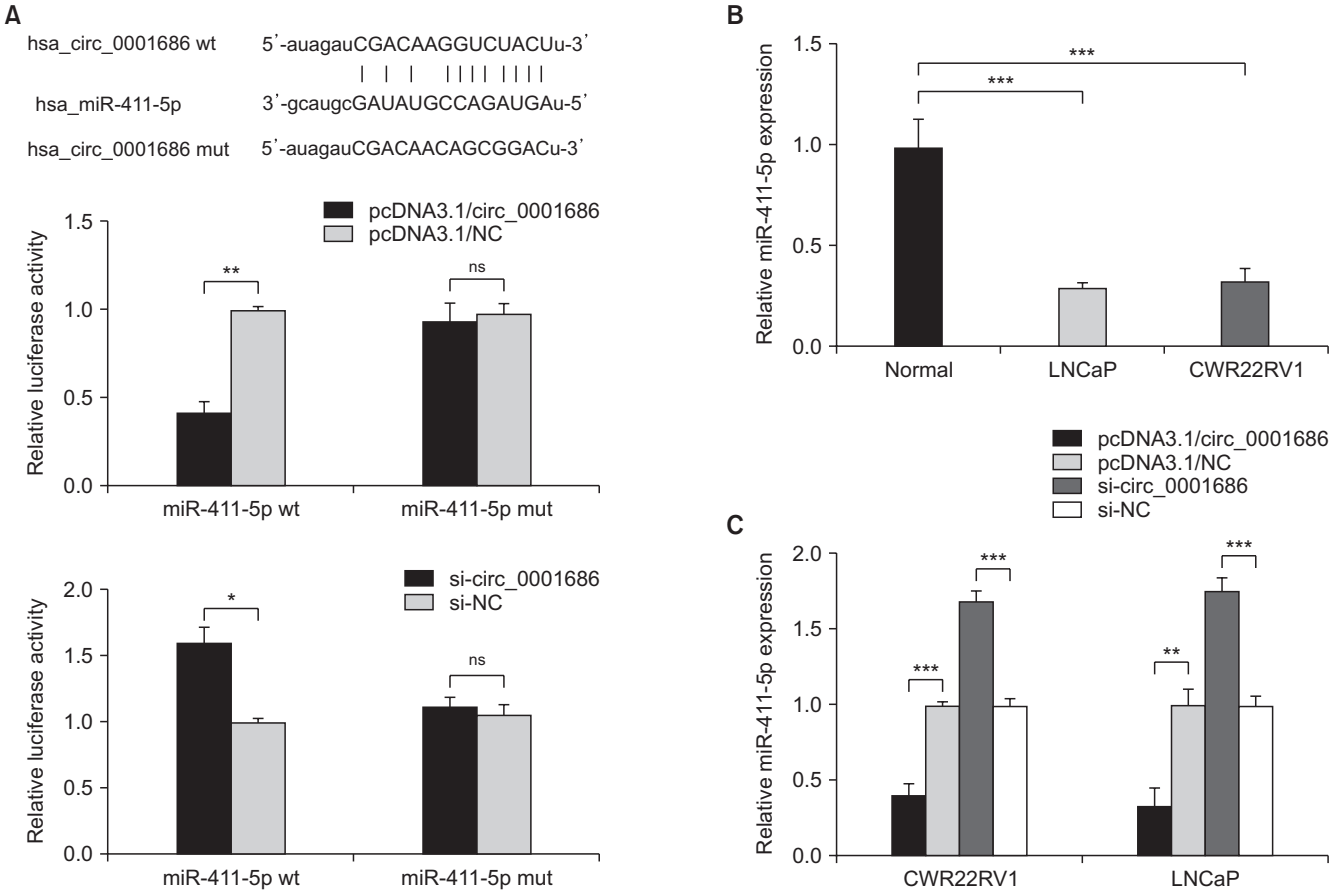

Fig. 3. Circ_0001686 directly binds to miR-411-5p in PCa cells. (A) The putative sequences of miR-411-5p and circ_0001686 with binding sites are shown. miR-411-5p significantly inhibited luciferase activity of wild type reporter for circ_0001686. (B) miR-411-5p was down-regulated by qRT-PCR detection in PCa cells (CWR22RV1 and LNCaP). (C) qRT-PCR was conducted to measure miR-411-5p expression in circ_0001686 transfected cells. PCa: prostate cancer, ns: not significant, wt: wild type, mut: mutant type. *p<0.05, **p<0.01, ***p<0.001.

(p<0.05, p<0.001; Fig. 4B), while this was increased by ASO-miR-411-5p (Fig. 4C). The migration and invasion of CWR22RV1 and LNCaP cells were suppressed by miR-411-5p (Fig. 4D, 4E), although miR-411-5p promoted apoptosis in the CWR22RV1 and LNCaP cells (p<0.01; Fig. 4F). In the PCa cells, the CD44 population was smaller in the miR-411-5p mimics group when compared to the mimics NC group, while in the control experiments, the CD44 population in the ASO-miR-411-5p group increased in comparison to the ASO-NC group (Fig. 4G).

5. miR-411-5p targeted SMAD3 and TGFBR2 in PCa cells

With a significantly high score, TargetScan predicted that the 3'-UTR of SMAD3 and TGFBR2 could be the target of miR-411-5p (Fig. 5A, 5B). Luciferase reporter assays results showed that miR-411-5p mimics decreased the luciferase activity of wild-type reporter vector carrying SMAD3 or TGFBR2, while ASO-miR-411-5p increased (Fig. 5A, 5B). qRT-PCR and western blot assays showed that miR-411-5p mimics inhibited the levels of SMAD3 and TGFBR2 in CWR22RV1 and LNCaP cells, both at the transcript and protein levels (Fig. 5C, 5D). Western blotting analysis and qRT-PCR results also showed that both the mRNA and protein levels of SMAD3 and TFRBR2 were increased upon pcDNA3.1/circ_0001686 transfection but decreased in si-circ_0001686 transfected CWR22RV1 and LNCaP cells (Fig. 5E, 5F). However, TGF-β reversed the level of SMAD3/TGFBR2 expression.

6. miR-411-5p suppresses prostate tumor growth and metastasis

CWR22RV1 cells transfected with miR-411-5p mimics or mimics NC were inoculated into male nude mice,

The World Journal of MEN's HEALTH

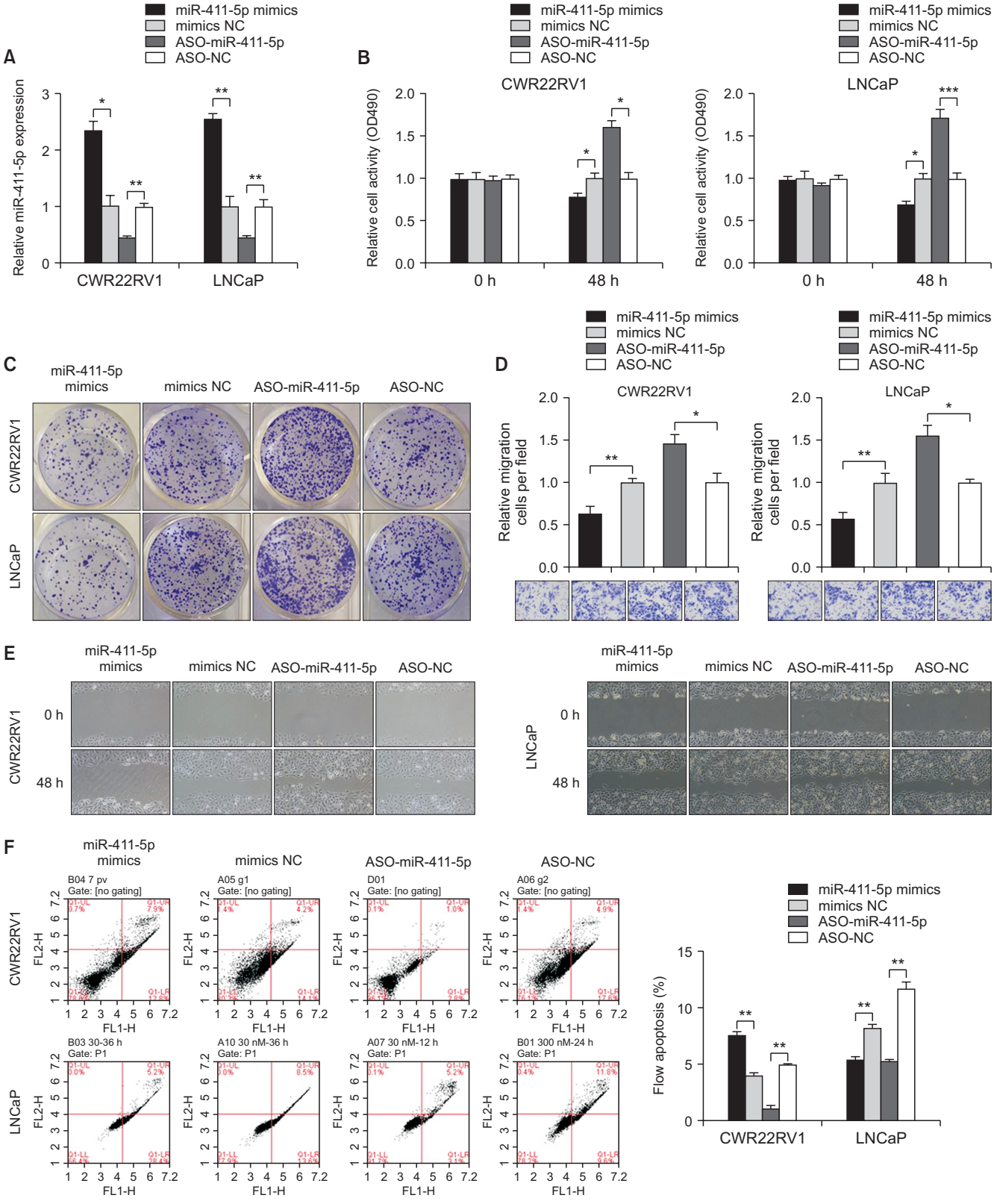

Fig. 4. miR-411-5p inhibits the proliferation, invasion of prostate cancer (PCa) cells. (A) miR-411-5p mimics, ASO-miR-411-5p were transfected into CWR22RV1 and LNCaP cells, and qRT-PCR was conducted to measure miR-411-5p expression. (B) The proliferation of cells transfected with miR-411-5p mimics, ASO-miR-411-5p detected by MTT assay. (C) miR-411-5p significantly suppressed the colony formation capacity of transfected cells. Transwell assay (×400) (D) and scratch wound assay (×200) (E) showed that miR-411-5p reduced the migration activity in CWR22RV1 and LNCaP cells (200 μm). (F) Apoptosis assay was performed by flow cytometry. (G) Flow cytometry analysis of CD44 expression in CWR22RV1 and LNCaP cells. *p<0.05, **p<0.01, ***p<0.001.

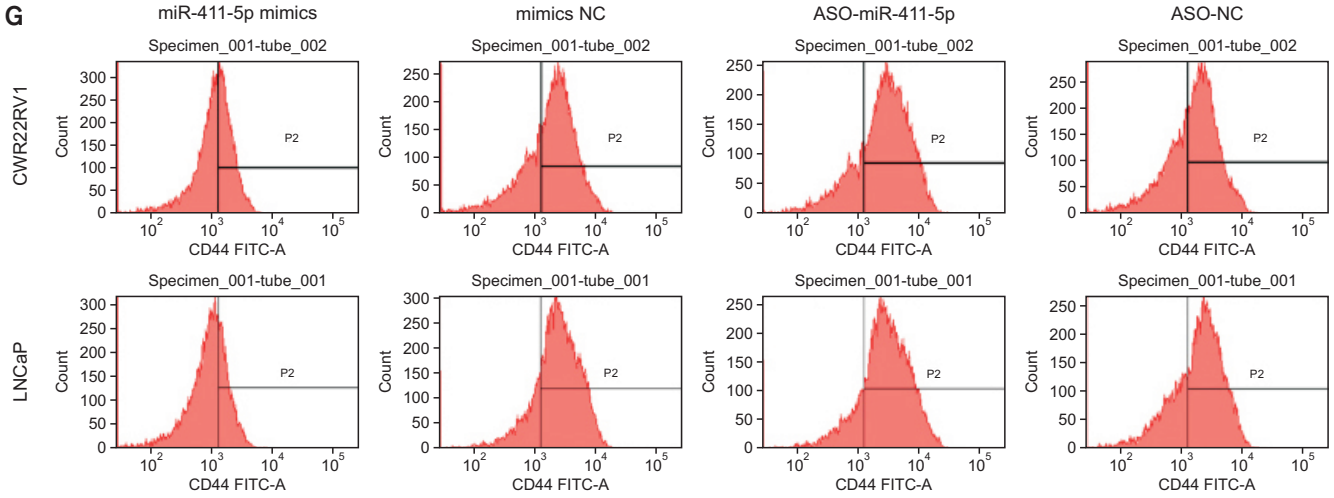

Fig. 4. Continued.

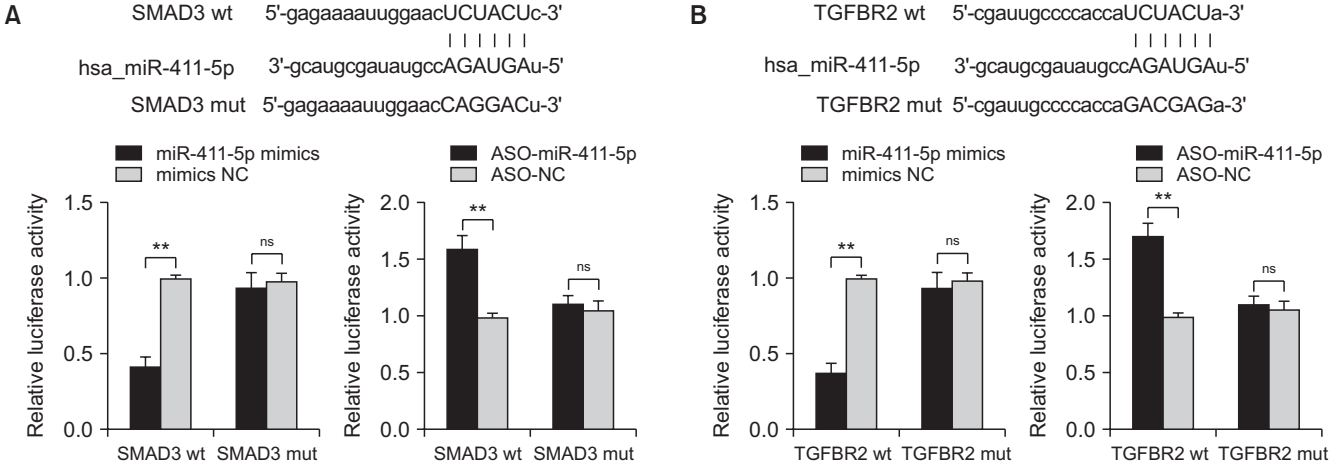

Fig. 5. miR-411-5p targets SMAD3 and TGFBR2 in prostate cancer (PCa) cells. (A, B) The putative sequence of miR-411-5p and SMAD3/TGFBR2 with binding sites. miR-411-5p significantly inhibited luciferase activity of wild type reporter for SMAD3/TGFBR2 in CWR22RV1 and LNCaP cells. (C) SMAD3 and TGFBR2 mRNA expression was down-regulated by miR-411-5p. (D) SMAD3 and TGFBR2 protein levels were down-regulated by miR-411-5p mimics. The mRNA (E) and protein (F) levels of SMAD3 and TGFBR2 were regulated by circ_0001686. PCa: prostate cancer, ns: not significant, wt: wild type, mut: mutant type. *p<0.05, **p<0.01, ***p<0.001.

and xenograft tumors were examined four weeks after the inoculation (Fig. 6A, 6B). We found that tumor volumes and weights in the miR-411-5p mimics group were significantly lower than those in the mimics NC group (Fig. 6C, 6D), strongly suggesting miR-411-5p could suppress tumorigenesis of PCa *in vivo*.

DISCUSSION

PCa carries the second-highest mortality rate in males, and finding a novel diagnostic marker is vital for the early screening of the disease. Importantly, CircRNAs are highly conserved and have a remarkably stable half-life of more than 48 hours, which makes them a promising tumor marker candidate in PCa diagnosis [20]. miRNAs are known to regulate many physiological and pathological processes in cancers. Interestingly, circRNAs are reported to function as a miRNA sponge, and their potential role in regulating cancer-related genes by fine-tuning target miRNAs has been recently recognized.

In this study, using qRT-PCR and microarray analysis, we found that circ_0001686 was significantly increased in PCa tissue and cell lines. Furthermore, the above results indicated that circ_0001686 could promote PCa cells proliferation, migration, and invasion, but miR-411-5p had the opposite effect. Based on these results, we found that circ_0001686 can interact

The World Journal of MEN's HEALTH

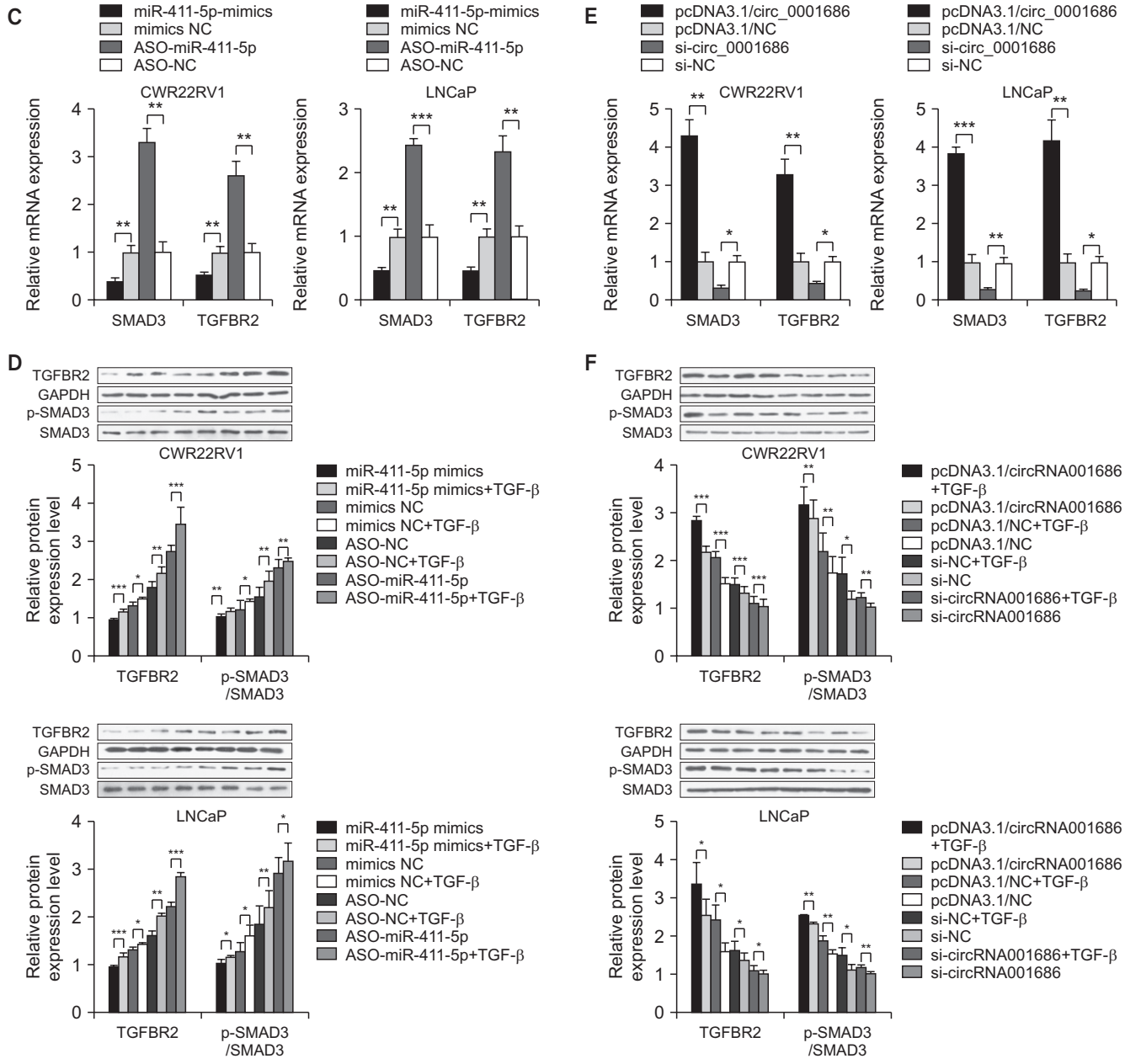

Fig. 5. Continued.

with miR-411-5p. As previous research has shown that circRNA can act as a sponge to sequester miRNA, our findings may be related to this mechanism of circRNA. Moreover, we also found that miR-411-5p down-regulated the levels of SMAD3 and TGFBR2.

The progression of PCa is a complex process regulated by multiple factors, and the TGF-β signaling pathway plays an important role in its occurrence and development. This may be because TGF-β can promote the epithelial-mesenchymal transformation (EMT) of tumor cells [21]. In the TGF-β signaling pathway, TGFBR2 binds to TGF-β, which then phosphorylates downstream targets. The activated kinase subsequently phosphorylates SMAD3 (p-SMAD3) to form a heteromeric complex with SMAD4 and is translocated into the nucleus to regulate the target gene's expression. This is critical for cell proliferation, differentiation, and apoptosis [17,21]. In our study, TGFBR2 and p-SMAD3 expression were also regulated by the miR-411-5p, and promoted the proliferation differentiation and migration of PCa cells. Furthermore, *in vivo* experiments also showed that miR-411-5p could inhibit PCa progression.

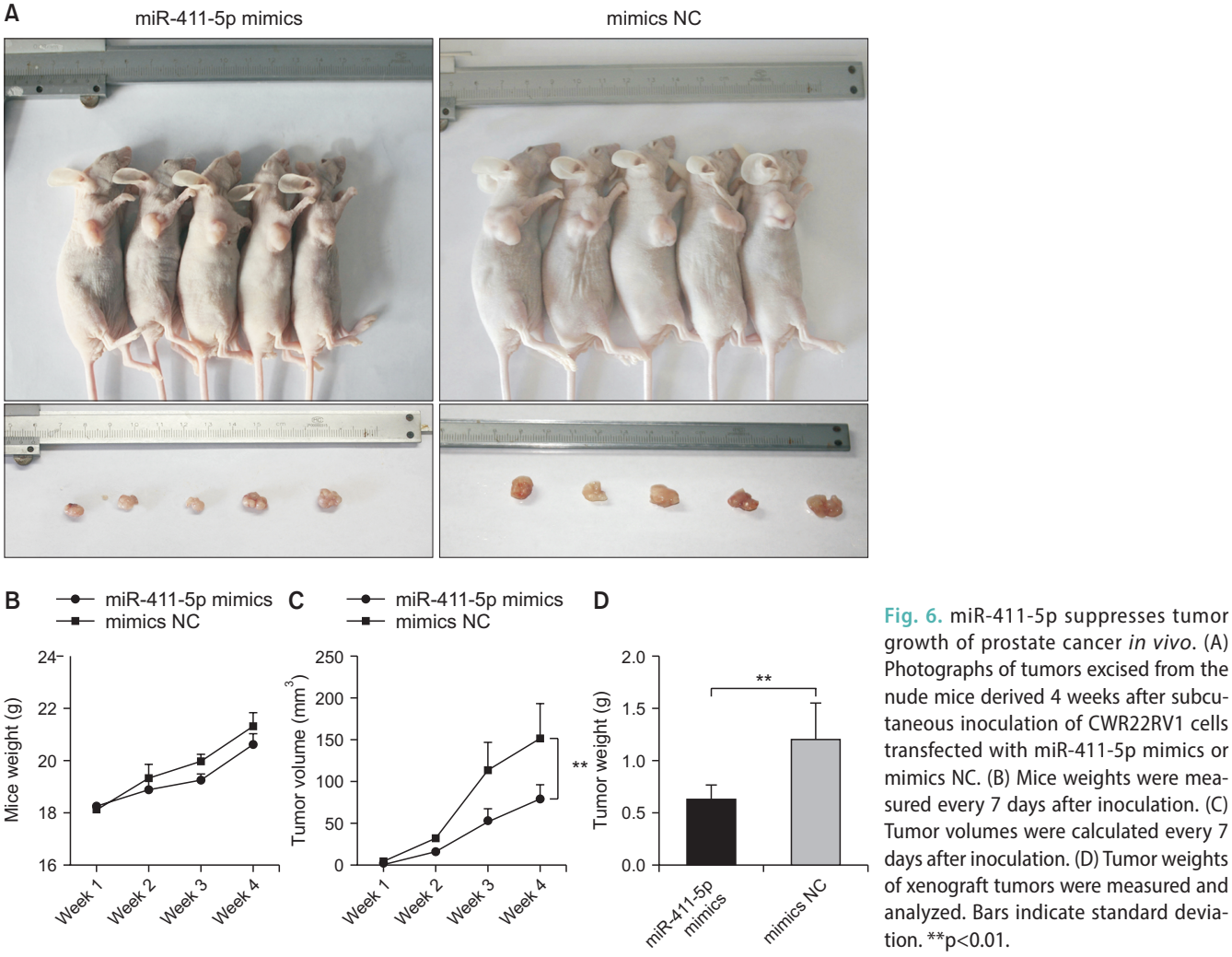

Fig. 6. miR-411-5p suppresses tumor growth of prostate cancer *in vivo*. (A) Photographs of tumors excised from the nude mice derived 4 weeks after subcutaneous inoculation of CWR22RV1 cells transfected with miR-411-5p mimics or mimics NC. (B) Mice weights were measured every 7 days after inoculation. (C) Tumor volumes were calculated every 7 days after inoculation. (D) Tumor weights of xenograft tumors were measured and analyzed. Bars indicate standard deviation. **p<0.01.

Although tumor progression cannot be attributed to epithelial-mesenchymal adaptive transformation, its role in the tumor progression mechanism cannot be ignored [22,23]. CD44+ tumor stem/progenitor cells are the intermediate bridge of the TGF-β -EMT signal pathway. A literature review found that down-regulated CD44 can inhibit cancer stem cell metastasis in PCa [24,25]. In the present study, we found that miR-411-5p mimics could suppress CD44 expression in CWR22RV1 and LNCaP cells suggesting miR-411-5p could function as a tumor suppressor in PCa [18,20,22]. The anti-PCa mechanisms elicited by carbon ion radiotherapy (CIRT) also involve exosomal miRNAs, including miR-411-5p [26]. A hypothetical model to summarize such regulation is depicted in Fig. 7.

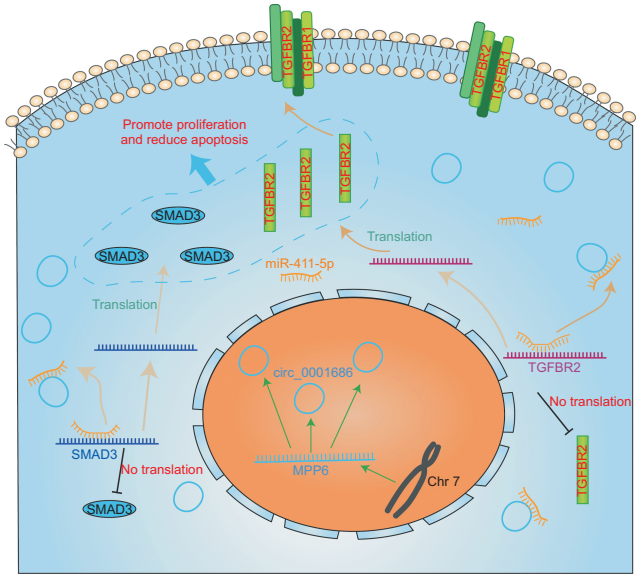

Fig. 7. The hypothetical model to summarize the mechanism of circ_0001686 induced tumor growth via miR-411-5p in prostate cancer.

CONCLUSIONS

Circ_0001686 can reduce the level of miR-411-5p and up-regulate TGFBR2/SMAD3 to promote PCa progression. This study's innovative findings demonstrate the interaction between circ_0001686 and miR-411-5p, which may assist the diagnosis and treatment of PCa in the future.

ACKNOWLEDGEMENTS

The authors thank all patients involved in this study.

This work was supported by The Science&Technology Development Fund of Tianjin Education Commission for Higher Education (grant number 2018KJ050).

Conflict of Interest

The authors have nothing to disclose.

Author Contribution

Conceptualization: QC, YC. Data curation: JP, ZL, EL, CF, DZ, ZY. Formal analysis: JP, XZ. Software: JP, DZ. Funding acquisition: QC. Writing – original draft: JP, DZ. Writing – review & editing: ZX, YN.

REFERENCES

1. Mohler JL, Armstrong AJ, Bahnson RR, D'Amico AV, Davis BJ, Eastham JA, et al. Prostate cancer, version 1.2016. J Natl Compr Canc Netw 2016;14:19-30.
2. Siegel RL, Miller KD, Jemal A. Cancer statistics, 2020. CA Cancer J Clin 2020;70:7-30.
3. Li T, Sun X, Chen L. Exosome circ_0044516 promotes prostate cancer cell proliferation and metastasis as a potential biomarker. J Cell Biochem 2020;121:2118-26.
4. Bolha L, Ravnik-Glavač M, Glavač D. Circular RNAs: biogenesis, function, and a role as possible cancer biomarkers. Int J Genomics 2017;2017:6218353.
5. Meng S, Zhou H, Feng Z, Xu Z, Tang Y, Li P, et al. CircRNA: functions and properties of a novel potential biomarker for cancer. Mol Cancer 2017;16:94.
6. Luan W, Shi Y, Zhou Z, Xia Y, Wang J. circRNA_0084043 promote malignant melanoma progression via miR-153-3p/Snail axis. Biochem Biophys Res Commun 2018;502:22-9.
7. Li P, Chen S, Chen H, Mo X, Li T, Shao Y, et al. Using circular RNA as a novel type of biomarker in the screening of gastric cancer. Clin Chim Acta 2015;444:132-6.
8. Liang HF, Zhang XZ, Liu BG, Jia GT, Li WL. Circular RNA circ-ABCB10 promotes breast cancer proliferation and progression through sponging miR-1271. Am J Cancer Res 2017;7:1566-76.
9. Huang G, Zhu H, Shi Y, Wu W, Cai H, Chen X. cir-ITCH plays an inhibitory role in colorectal cancer by regulating the Wnt/β-catenin pathway. PLoS One 2015;10:e0131225.
10. Dai Y, Li D, Chen X, Tan X, Gu J, Chen M, et al. Circular RNA myosin light chain kinase (MYLK) promotes prostate cancer progression through modulating Mir-29a expression. Med Sci Monit 2018;24:3462-71.
11. Xiang Z, Xu C, Wu G, Liu B, Wu D. CircRNA-UCK2 increased TET1 inhibits proliferation and invasion of prostate cancer cells via sponge MiRNA-767-5p. Open Med (Wars) 2019;14:833-42.
12. Chen LL. The biogenesis and emerging roles of circular RNAs. Nat Rev Mol Cell Biol 2016;17:205-11.
13. Bartel DP. MicroRNAs: target recognition and regulatory functions. Cell 2009;136:215-33.
14. Bueno MJ, Pérez de Castro I, Malumbres M. Control of cell proliferation pathways by microRNAs. Cell Cycle 2008;7:3143-8.
15. Cummins JM, Velculescu VE. Implications of micro-RNA profiling for cancer diagnosis. Oncogene 2006;25:6220-7.
16. Liu Y, Liu T, Jin H, Yin L, Yu H, Bi J. MiR-411 suppresses the development of bladder cancer by regulating ZnT1. Onco Targets Ther 2018;11:8695-704.
17. Finnson KW, Chi Y, Bou-Gharios G, Leask A, Philip A. TGF-b signaling in cartilage homeostasis and osteoarthritis. Front Biosci (Schol Ed) 2012;4:251-68.
18. Livak KJ, Schmittgen TD. Analysis of relative gene expression data using real-time quantitative PCR and the 2(-Delta Delta C(T)) method. Methods 2001;25:402-8.
19. Xia Q, Ding T, Zhang G, Li Z, Zeng L, Zhu Y, et al. Circular RNA expression profiling identifies prostate cancer-specific circRNAs in prostate cancer. Cell Physiol Biochem 2018;50:1903-15.
20. Bai TL, Liu YB, Li BH. MiR-411 inhibits gastric cancer proliferation and migration through targeting SETD6. Eur Rev Med Pharmacol Sci 2019;23:3344-50.
21. Bedan M, Grimm D, Wehland M, Simonsen U, Infanger M, Krüger M. A focus on macitentan in the treatment of pulmonary arterial hypertension. Basic Clin Pharmacol Toxicol 2018;123:103-13.
22. Garber K. Epithelial-to-mesenchymal transition is important to metastasis, but questions remain. J Natl Cancer Inst

2008;100:232-3, 239.
23. Thompson EW, Williams ED. EMT and MET in carcinoma--clinical observations, regulatory pathways and new models. Clin Exp Metastasis 2008;25:591-2.
24. Liu C, Kelnar K, Liu B, Chen X, Calhoun-Davis T, Li H, et al. The microRNA miR-34a inhibits prostate cancer stem cells and metastasis by directly repressing CD44. Nat Med 2011;17:211-5.
25. Senbanjo LT, Chellaiah MA. CD44: a multifunctional cell surface adhesion receptor is a regulator of progression and metastasis of cancer cells. Front Cell Dev Biol 2017;5:18.
26. Yu Q, Li P, Weng M, Wu S, Zhang Y, Chen X, et al. Nanovesicles are a potential tool to monitor therapeutic efficacy of carbon ion radiotherapy in prostate cancer. J Biomed Nanotechnol 2018;14:168-78.